Electron Transfer through the Hydrogen-Bonded Interface of a β-Turn-Forming Depsipeptide

David A. Williamson† and Bruce E. Bowler*

Contribution from the Department of Chemistry and Biochemistry, 2190 East Iliff Avenue, University of Denver, Denver, Colorado 80208-2436

Received April 22, 1998

Abstract: Hydrogen-bonding networks are believed to play an important role in electron-transfer pathways in a protein medium. A porphyrin−quinone donor−acceptor compound with a depsipeptide bridge which forms a β-turn has been synthesized to study hydrogen bond-mediated electron transfer. The placement of the donor and acceptor has been chosen to favor electron transfer through the hydrogen bond interface of the β-turn. Use of ester linkages also allows control of the hydrogen-bonding pattern within the β-turn-forming depsipeptide. Infrared spectroscopy in the amide A (NH stretch) and amide I (carbonyl stretch) regions indicates that the β-turn conformation is about 85% populated in dichloromethane and essentially completely disrupted in dimethyl sulfoxide at 296 K. The electron-transfer rate constant, k_{et}, was evaluated using the singlet excited-state lifetimes of the porphyrin in the presence and absence of an electron acceptor. The lifetimes were obtained using time-correlated single-photon-counting fluorescence spectroscopy. Very fast electron transfer ($k_{et} = (1.1 \pm 0.1) \times 10^9$ s^{-1}) was observed in the presence of the β-turn conformation. When the β-turn structure was disrupted using the solvent DMSO, electron transfer was no longer competitive with the intrinsic fluorescence emission. Analysis of the data in terms of Marcus theory and the pathway model for electronic coupling yielded a value for the hydrogen bond coupling decay factor, ϵ_{hb}, of 0.8 ± 0.4, which is of the same order of magnitude as the theoretically predicted value of 0.36.

Introduction

Long-range electron transfer has been studied extensively in proteins,[1] protein−protein complexes,[2] models for photosynthetic reaction centers,[3] and peptides,[4] including recent work with peptides that mimic β-sheet structure.[5] Outer-sphere electron transfer is a function of nuclear position, electronic coupling, driving force, medium, and electron donor and electron acceptor spatial arrangement. The Marcus equation (see eq 1)[6] relates these factors to the rate constant for electron transfer, k_{et}. Some studies indicate that electronic coupling between the electron donor and electron acceptor decays exponentially, scaled by a constant factor, β, indicative of a homogeneous electronic coupling medium (see eq 2).[7] Dutton and co-workers

$$k_{et} = \left(\frac{\pi}{\hbar^2 \lambda k_B T}\right)^{1/2} [H_{ab}]^2 \, e^{-[(\Delta G^\circ + \lambda)^2/4\lambda k_B T]} \quad (1)$$

$$k_{et} \propto [H_{ab}]_o^{\,2} \, e^{-(\beta R)} \quad (2)$$

report $\beta = 1.4$ Å^{-1} for proteins,[7] in line with the theoretical prediction of Hopfield.[8] In the pathway model, developed by Beratan and Onuchic,[9] electron transfer between the donor and acceptor is expected to have structure-dependent inhomogeneities and thus will not depend smoothly on through-space distance. In this model, the electronic coupling matrix element, H_{ab}, has contributions from different types of orbital interactions—through bond, through space, and through hydrogen bond. Each type of orbital interaction is represented by a decay constant (ϵ_c, ϵ_{ts}, and ϵ_{hb}, respectively), which reflects the magnitude of the decrease of electronic coupling across that type of orbital interaction. Electronic coupling through hydrogen bonds is important to understand in the case of protein electron transfer due to the prevalence of hydrogen bond networks in proteins. Several studies have demonstrated that hydrogen bonds can mediate electron transfer efficiently,[10] although the exact nature

† Present address: Department of Chemistry, University of Kansas, Lawrence, KS 66045.

(1) (a) Wuttke, D. S.; Bjerrum, M. J.; Winkler, J. R.; Gray, H. B. *Science* **1992**, *256*, 1007−1009. (b) Mayo, S. L.; Ellis, W. R., Jr.; Crutchley, R. J.; Gray, H. B. *Science* **1986**, *233*, 948−952. (c) Bowler, B. E.; Raphael, A. L.; Gray, H. B. *Prog. Inorg. Chem.* **1990**, *38*, 259−322. (d) Langen, R.; Chang, I.-J.; Germanas, J. P.; Richards, J. H.; Winkler, J. R.; Gray, H. B. *Science* **1995**, *268*, 1733−1735. (e) Gray H. B.; Winkler, J. R. *Annu. Rev. Biochem.* **1996**, *65*, 537−561.

(2) Nocek, J. M.; Zhou, J. S.; De Forest, S.; Priyadarshy, S.; Beratan, D. N.; Onuchic, J. N.; Hoffman, B. M. *Chem. Rev.* **1996**, *96*, 2459−2489.

(3) (a) Moore, T.; Gust, D. *Adv. Photochem.* **1991**, *16*, 1−64. (b) Meyer, T. J. *Acc. Chem. Res.* **1989**, *22*, 163−170.

(4) (a) Isied, S. In *Electron Transfer in Inorganic, Organic, and Biological Systems*; Bolton, J., Mataga, N., McLendon, G., Eds.; ACS Advances in Chemistry Series 228; American Chemical Society: Washington, DC, 1991; pp 229−245. (b) Isied, S. In *Electron-Transfer Reactions: Inorganic, Organometallic, and Biological Applications*; Isied S., Ed.; ACS Advances Chemistry Series 253; American Chemical Society: Washington, DC, 1997; pp 331−347.

(5) (a) Gretchikhine, A. B.; Ogawa, M. Y. *J. Am. Chem. Soc.* **1996**, *118*, 1543−1544. (b) Fernando, S. R. L.; Kozlov, G. V.; Ogawa, M. Y. *Inorg. Chem.* **1998**, *37*, 1900−1905.

(6) Marcus, R. A.; Sutin, N. *Biochim. Biophys. Acta* **1985**, *811*, 266−273.

(7) Moser, C. C.; Keske, J. M.; Warncke, K.; Farid, R. S.; Dutton, L. P. *Science* **1992**, *355*, 796−802.

(8) Hopfield, J. J. *Proc. Nat. Acad. Sci. U.S.A.* **1974**, *71*, 3640−3644.

(9) Onuchic, J. N.; Beratan, D. N.; Winkler, J. R.; Gray, H. B. *Annu. Rev. Biophys. Biomol. Struct.* **1992**, *21*, 349−377.

(10) (a) de Rege, P. J. F.; Williams, S. A.; Therien, M. J. *Science* **1995**, *269*, 1409−1413. (b) Turro, C.; Chang, C. K.; Leroi, G. E.; Cukier, R. I.; Nocera, D. G. *J. Am. Chem. Soc.* **1992**, *114*, 4013−4015. (c) Kirby, J. P.; Roberts, J. A.; Nocera, D. G. *J. Am. Chem. Soc.* **1997**, *119*, 9230−9236. (d) Roberts, J. A.; Kirby, J. P.; Wall, S. T.; Nocera, D. G. *Inorg. Chim. Acta* **1997**, *263*, 395−405.

10.1021/ja981384k CCC: $15.00
Published on Web 10/09/1998

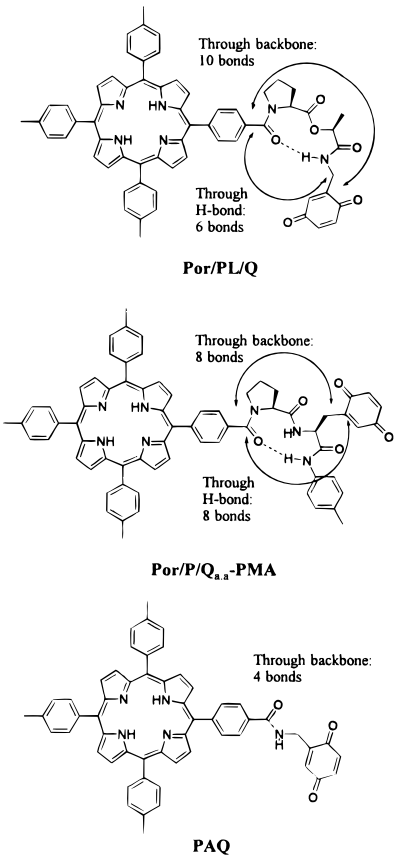

Figure 1. Structures of porphyrin−quinone donor−acceptor compounds. Por/PL/Q and Por/P/Q_{aa}-PMA[11] both form β-turn structures. PAQ[12,13] connects the donor and acceptor used in Por/PL/Q directly via an amide bond. The through-bond electron-transfer pathways between the edge of the tritolyl-*p*-carboxyphenylporphyrin donor and the edge of the quinone acceptor are indicated on each structure. A shared hydrogen between two heteroatoms is counted as two bonds.

of the hydrogen-bonded interface can alter this efficiency dramatically.[10b,d]

In the work described here, a donor−acceptor compound with a β-turn-forming depsipeptide bridge (Por/PL/Q in Figure 1) has been developed to study hydrogen bond-mediated electron transfer through a single amide NH to amide carbonyl (NH- - -O═C) peptide hydrogen bond. Tamiaki and Muruyama have previously reported electron-transfer studies with a donor−acceptor compound bridged by a β-turn-forming peptide (Por/P/Q_{aa}-PMA in Figure 1).[11] An advantage of the depsipeptide bridge used in Por/PL/Q is that the central amide linkage has been replaced with an ester, ensuring β-turn folding (C_{10} turn) and eliminating the possibility of γ-turn folding (C_7 turn). The shortest "pathway" that results passes through the hydrogen bond and has fewer bonds than the pathways possible for Por/P/Q_{aa}-PMA. Por/PL/Q can also be compared to electron transfer in the compound PAQ (see Figure 1), reported on previously by Bolton and co-workers.[12,13] The donor porphyrin and acceptor quinone are identical to those used in Por/PL/Q. Relative to PAQ, the shortest through-bond pathway of Por/PL/Q has had the NH- - -O═C hydrogen bond inserted into it. Also, three of the four covalent bonds in the shortest pathways of PAQ and Por/PL/Q are identical. Thus, comparison of the electron-transfer properties of Por/PL/Q and PAQ should allow the effect of a single hydrogen bond on electronic coupling to be evaluated in a straightforward way.

The organic solvent of choice for a β-turn-forming peptide must be a non-hydrogen-bonding solvent so that hydrogen bond formation is favored. Electron transfer has been studied in hydrogen bond-promoting and hydrogen bond-disrupting solvents. Thus, electron transfer in the presence and absence of the hydrogen bond interface shown in Figure 1 for Por/PL/Q has been evaluated.

Experimental Section

tBoc-L-Proline-L-lactate-*N*-2,5-dimethoxybenzylamide (tBoc/PL/DMB), porphyrin-L-proline-L-lactate-*N*-2,5-dimethoxybenzylamide (Por/PL/DMB), the *p*-benzoquinone form of Por/PL/DMB, Por/PL/Q (Figure 1), and the non-hydrogen-bonding IR standard, *N*-methyl-D-5-oxoproline methyl amide (NPMA), were synthesized according to Williamson and Bowler.[14] Tetrahydrofuran (THF) was dried on molecular sieves and then distilled from sodium benzophenone ketyl and stored on molecular sieves. *N*,*N*-Dimethylformamide (DMF) was stored on anhydrous $MgSO_4$ before distillation under reduced pressure. Triethylamine was distilled from sodium benzophenone ketyl and stored on KOH pellets to maintain dryness. All other chemicals were reagent grade or better. Two other IR standards were prepared as follows.

Methyl-1-acetyl-2-L-pyrrolidinecarboxylate (MAPC). L-Proline (3.00 g, 26.1 mmol) was dissolved in dry methanol (15 mL) and stirred at −20 °C (ice/salt bath). Thionyl chloride (7 mL) was added to the slurry over a 1-h period with an addition funnel. The reaction was stirred for an additional 6 h. After all the solids were dissolved, the reaction was concentrated to dryness. The resulting yellow oil was dissolved in toluene (50 mL) and concentrated to dryness by rotary evaporation to remove residual thionyl chloride and methanol. The oil was dried overnight under vacuum. It was then dissolved in dry DMF (10 mL) containing triethylamine (4 mL) and stirred on an ice bath. Acetyl chloride (2.3 mL, 32 mmol) was dissolved in dry THF (50 mL) and added dropwise with an addition funnel over a period of 1 h. The reaction mixture was stirred overnight under a $CaCl_2$ drying tube. The mixture was diluted with dichloromethane (250 mL) and was extracted with $NaHSO_4$ (3 × 250 mL), saturated sodium bicarbonate (250 mL), and brine (250 mL). The organic layer was dried with anhydrous sodium sulfate and concentrated by rotary evaporation, yielding 3.77 g (84.5%) of a brown oil. ^{1}H NMR ($CDCl_3$): δ 1.97−2.20 (4 H, m), 2.01 and 2.10 (3 H, two singlets), 3.5−3.75 (2 H, m) 3.75 (3 H, d), 4.44 (1 H, dd).

Methyl-1-benzoyl-2-L-pyrrolidinecarboxylate (MBPC). Procedure was identical to the synthesis of methyl-1-acetyl-2-L-pyrrolidine carboxylate, except benzoyl chloride (3.2 mL, 27 mmol) was used instead of acetyl chloride. Yield of a light yellow solid was 4.29 g (68.6%), mp 83 °C. ^{1}H NMR ($CDCl_3$): δ 2.00−2.30 (4 H, m), 3.57−3.65 (2 H, m), 3.75 (3 H, s), 4.70 (1 H, t), 7.42−7.57 (5H, m).

Temperature-Dependent Amide NH NMR Spectra. Temperature-dependent NMR studies were carried out in 99.9% dichloromethane-d_2 (Isotec, Miamisburg, OH). All chemical shifts are reported in ppm and are referenced to the residual solvent peak (CH_2Cl_2 = 5.32 ppm). Carbon tetrachloride was spectroscopic grade purchased from Mallinckrodt and was distilled from Al_2O_3 before use. All chemical shifts in carbon tetrachloride are reported in ppm and are referenced to tetramethylsilane (TMS = 0.0 ppm). All ^{1}H NMR data were obtained using a Chemagnetics 200-MHz FT-NMR operating at 199.167 MHz. Temperature was controlled with a Chemagnetics REX-C_{1000} temperature controller. The temperature was calibrated with methanol according to Van Geet.[15] The methanol shifts reported by Van Geet and the methanol shifts observed on the Chemagnetics 200-MHz NMR spectrometer were coincident as a function of temperature. Therefore, temperature was read directly from the Chemagnetics temperature

(11) Tamiaki, H.; Maruyama, K. *Chem. Lett.* **1993**, 1499−1502.
(12) (a) Archer, M. D.; Gadzepko, V. P. Y.; Bolton, J. R.; Schmidt, J. A.; Weedon, A. C. *J. Chem. Soc., Faraday Trans. 2* **1986**, *82*, 2305−2313. (b) Schmidt, J. A.; Liu, J.-Y.; Bolton, J. R.; Archer, M. D.; Gadzekpo, V. P. Y. *J. Chem. Soc., Faraday Trans. 1* **1989**, *85*, 1027−1041.
(13) Lui, J.-Y.; Schmidt, J. A.; Bolton, J. R. *J. Phys. Chem.* **1991**, *95*, 6924−6927.
(14) Williamson, D. A.; Bowler, B. E. *Tetrahedron* **1996**, *52*, 12357−12372.
(15) Van Geet, A. L. *Anal. Chem.* **1970**, *42*, 679−680.

controller without correction. Before sample preparation, all samples were dried on a drying pistol using KOH pellets as a drying agent and refluxing methanol for heat. All samples were prepared as approximately 1.0 mM solutions and were stored in the dark. The chemical shift of the amide NH as a function of temperature was fit to a linear equation to obtain the rate of change of the amide NH chemical shift with respect to temperature, $\Delta\delta$NH/ΔT. The correlation coefficient, r^2, was greater than 0.99 in all cases.

Amide A and Amide I Infrared Spectra. FTIR studies were carried out in anhydrous dichloromethane (DCM) or dimethyl sulfoxide (DMSO), which were purchased from Aldrich at 99.98% purity in sure seal bottles. DCM was treated with anhydrous K_2CO_3 to remove any residual water or acid. Infrared spectral data were obtained with a Nicolet Protégé 460 FT-IR spectrometer at 2-cm^{-1} resolution and are reported in cm^{-1}. The spectrometer was purged with dry N_2 for 15 min before spectra were recorded. Samples were prepared between CaF_2 plates with a 1.0-mm path length spacer. All spectra were processed using OMNIC (ver. 2.1) software by subtraction of the solvent background (using the optically clear region near 2000 cm^{-1}), subtraction of residual water vapor, and baseline correction. Curve-fitting was carried out using Grams/386 (ver. 3.02) software. Curve-fitting routines were stopped when a minimum χ^2 value was obtained for the anticipated number of stretches, and the curve fit resembled the actual spectrum by visual inspection. Residual line correlations (R^2) were better than 0.995. If the curve fit for the anticipated number of peaks did not resemble the peak profile, additional peaks were added until the fit resembled the peak profile. Normally, a mixed Gaussian and Lorentzian curve shape was used to represent the IR absorption bands in the curve-fitting procedure. If the fit for a particular curve was either 100% Lorentzian or Gaussian, the peak was fixed as such, and curve-fitting for the other curves was allowed to continue using mixed functions. All compounds were dried on a drying pistol as described above for NMR samples. DCM and DMSO samples were prepared at a concentration of ~1 mM in a drybox flushed with dry N_2.

Temperature-Dependent Amide A IR Measurements. For temperature-dependent IR studies in DCM, A Nicolet 5DXC FTIR spectrometer was used at a resolution of 4 cm^{-1}. A cold head with KBr windows (RMC Cryosystems, model 22, Tucson, AZ), equipped with a He compressor and a gold-plated liquid sample holder, was used. Samples were placed in a 1-cm path length IR quartz cell (International Crystal Labs, Inc., Garfield, NJ), which was sealed with a Teflon lid and Parafilm to prevent solvent evaporation. A Palm Beach Cryophysics, Inc. series 4000 cryogenic thermometer/controller was used to control and monitor the temperature within the cold head. The temperature was allowed to equilibrate for 20 min before each spectrum was acquired. Spectra were processed as above for room-temperature data. The non-hydrogen-bonding standard, NPMA, was used to evaluate the extinction coefficient for the non-hydrogen-bonded secondary amide NH stretching vibration at 3445 cm^{-1} as a function of temperature. This extinction coefficient was then used to evaluate the equilibrium constant for β-turn formation at each temperature, $K_{\beta-\mathrm{turn}}(T)$, for Por/PL/DMB, using eq 3, where $[\mathrm{Por/PL/DMB}]_{\mathrm{total}}$ is the total

$$K_{\beta-\mathrm{turn}}(T) = \{[\mathrm{Por/PL/DMB}]_{\mathrm{total}} - (\mathrm{Abs}_{\mathrm{NHB-Por/PL/DMB}}(T)/\epsilon_{\mathrm{NPMA}}(T))\}/(\mathrm{Abs}_{\mathrm{NHB-Por/PL/DMB}}(T)/\epsilon_{\mathrm{NPMA}}(T)) \quad (3)$$

concentration of Por/PL/DMB in the sample, $\mathrm{Abs}_{\mathrm{NHB-Por/PL/DMB}}(T)$ is the absorbance at the non-hydrogen-bonding NH stretching frequency (~3445 cm^{-1}) of Por/PL/DMB at temperature T, and $\epsilon_{\mathrm{NPMA}}(T)$ is the extinction coefficient of the stretching vibration of the secondary amide NH of NPMA, the non-hydrogen-bonding standard, at temperature T.

ROESY ^{1}H NMR Experiments. The 2D ROESY experiment[16] on Por/PL/DMB was performed on a Varian 500-MHz NMR spectrometer in the Department of Chemistry and Biochemistry at the University of Colorado at Boulder. Por/PL/DMB was dissolved in CD_2Cl_2, freeze−pump−thawed (five cycles) to remove O_2, and refilled with N_2. The NMR tube was then sealed with an O_2 torch. During spectral acquisition, the sample temperature was controlled at 5.0 °C. The spectrum was obtained with $\tau_1 = 300$ μs (150 increments, 96 scans/increment), $\tau_2 = 100$ μs (4096 points), $\tau_m = 0.25$ s with a spin lock pulse of ~2 kHz, a delay time of 1.2 s, and a spectral width of 12 kHz. Data were analyzed with Felix (ver. 95.0) software.

Fluorescence Lifetime Measurements. The time-correlated single-photon-counting (TCSPC) experiments[17] were performed at the Beckman Institute's Laser Resource Center (California Institute of Technology, Pasadena, CA). TCSPC fluorescence decay curves were produced by the buildup of a histogram of counts versus time. A mode-locked, synchronously pumped, cavity-dumped dye laser was used to photoexcite the sample at 600 nm (60 mW, 3.8 MHz, and 12 ps pulse width). The fluorescence emission was passed through a polarizer set at the magic angle of 54.7°. The light then entered a monochromator, which was set at 650 nm. The histograms obtained were fit to single- or multiple-exponential decays using curve-fitting software developed at Caltech and based upon least-squares methods. The fit was believed to be appropriate for the decay when $\chi_\nu^2 \approx 1.0$, where χ_ν^2 is chi-squared normalized to the number of degrees of freedom. The samples for the TCSPC experiments were dried overnight in a drying pistol as for the temperature-dependent NMR experiments. The samples were prepared at a concentration of 2−10 μM in a 1-cm quartz fluorescence cell, which was attached to a 10-mL Pyrex volumetric flask and a Teflon stopcock. After the dried samples were dissolved into anhydrous dichloromethane or dimethyl sulfoxide, the samples were freeze−pump−thawed in the attached Pyrex flask a minimum of 10 cycles to remove dioxygen. The degree of oxidation of the quinone moiety of Por/PL/Q was estimated from the increase in the extinction coefficient at 248 nm ($\epsilon_{248} = 20\,300$ M^{-1} cm^{-1} for methyl-*p*-benzoquinone in CH_2Cl_2)[18] relative to Por/PL/DMB.

Calculation of Rate Constants, Driving Force, and Reorganization Energies. Electron-transfer rate constants, k_{et}, were calculated using eq 4,[19] where τ_o is the fluorescence lifetime for Por/PL/DMB

$$k_{\mathrm{et}} = \frac{1}{\tau_1} - \frac{1}{\tau_0} \quad (4)$$

and τ_1 is the lifetime for Por/PL/Q. It is assumed that electron transfer is the only additional excited-state decay pathway introduced in the conversion from Por/PL/DMB to Por/PL/Q. Energy transfer is not expected to compete since there is no spectral overlap between the porphyrin emission near 650 nm and quinone absorbance bands.

The driving force ($-\Delta G°$) for a free base Por/PL/Q molecule in dichloromethane was calculated using eq 5. This equation has been

$$\Delta G° = e(E_{\mathrm{P}}° - E_{\mathrm{Q}}°) - \frac{e^2}{4\pi\epsilon_o\epsilon_s a_{\mathrm{PQ}}} - \Delta G_{\mathrm{ES}} \quad (5)$$

found to successfully correlate electron-transfer rate constants for porphyrin−quinone donor−acceptor compounds in a variety of solvents.[12] The values for $E_{\mathrm{P}}°$ and $E_{\mathrm{Q}}°$, the electrochemical potentials for one-electron oxidation of free base porphyrin and the one-electron reduction of quinone, respectively, are taken from previously published electrochemical data for the porphyrin and quinone moieties used in Por/PL/Q.[12] Since $E_{\mathrm{P}}°$ and $E_{\mathrm{Q}}°$ were not reported for DMSO in the previous work,[12] the CH_3CN values were used, since $\epsilon_s(CH_3CN)$ is similar to ϵ_s(DMSO). $E_{\mathrm{P}}°-E_{\mathrm{Q}}°$ values in a wide range of solvents deviate from the value of 1.41 eV in CH_3CN by ±0.1 eV. We have used this deviation to define the error in the evaluation of $-\Delta G°$ for DMSO and propagated this error into subsequent calculations. The second term in eq 5 is a Coulombic correction to account for stabilization of the charge-transfer state produced after electron transfer. In the second term, ϵ_o is the permittivity of free space (8.854×10^{-12} C^2 N^{-1} m^{-2}). The static dielectric constants used were ϵ_s(DCM) =

(16) Bothner-By, A. A.; Stephen, R. L.; Lee, J.; Warren, C. D.; Jeanloz, R. W. *J. Am. Chem. Soc.* **1984**, *160*, 811−813.

(17) Small, E. W. In *Topics in Fluorescence Spectroscopy, Vol. 1: Techniques*; Lakowicz, J. R., Ed.; Plenum Press: New York, 1991; pp 97−182.

(18) McIntosh, A. R.; Siemiarczuk, A.; Bolton, J. R.; Stillman, M. J.; Ho, T.-F.; Weedon, A. C. *J. Am. Chem. Soc.* **1983**, *105*, 7125−7223.

(19) Lakowicz, J. R. *Principles of Fluorescence Spectroscopy*; Plenum Press: New York, 1983; pp 261−262.

8.93 and ϵ_s(DMSO) = 46.68 (refs 20a,b, respectively). The distance between the donor and acceptor, a_{PQ}, was estimated using the molecular modeling program HyperChem (ver. 3.0). To obtain a_{PQ}, a conformational search was carried out about the dihedral angles on either side of the methylene group connecting the quinone to the β-turn. A type I β-turn was assumed on the basis of IR data (see Discussion section; for Φ,Ψ conformational angles, see ref 21). The tolyl and *p*-carboxyphenyl groups were assumed to be perpendicular to the porphyrin ring, and the carboxy group that connects the porphyrin system to the proline was assumed to be perpendicular to the benzene ring it is attached to. The center-to-center distance from the porphyrin to the quinone for each conformation within 5 kcal/mol of the lowest energy conformation was used to calculate a weighted average value of a_{PQ}. The weighting for each distance was based on the Boltzmann population of each conformation expected from its energy relative to the lowest energy conformation. Energies were calculated with the mm+ force field[22] provided with HyperChem. We have assumed that the porphyrin and quinone moieties do not significantly perturb the depsipeptide β-turn backbone angles. For the β-turn formed by Por/PL/Q, a value of a_{PQ} = 9.8 Å was obtained. The range of distances within a Boltzmann weighting ≥0.1 is 8.7−10.7 Å. The third term in eq 5, ΔG_{ES}, is the free energy of the excited state and was calculated using eq 6,[23] where E_0 is the energy of the fluorescence maximum (657 nm) of Por/PL/DMB and χ' is the reorganization energy due to solvent and low-frequency vibrational modes. χ' is given by eq 7, where $\Delta\bar{\nu}_{0,1/2}$

$$\Delta G_{ES} = E_0 + \chi' \tag{6}$$

$$\chi' = \frac{(\Delta\bar{\nu}_{0,1/2})^2}{(16k_BT\ln 2)} \tag{7}$$

is the full width of the emission band at half-maximum. Both E_0 and χ' are enthalpic quantities. The use of this equation to represent the free energy of the excited state is justified by the negligible pressure−volume work[23b] expected in solution and the small contribution expected from the electronic entropic change.[23a]

The reorganization energy ($\lambda = \lambda_s + \lambda_i$) was calculated from the solvent reorganization energy (λ_s) using eq 8[6] and an internal reorganizational energy (λ_i) of 0.2 eV.[12,13] Values for ϵ_{op} were obtained from

$$\lambda_s = \frac{(\Delta e)^2}{4\pi\epsilon_o}\left(\frac{1}{2a_P} + \frac{1}{2a_Q} - \frac{1}{a_{PQ}}\right)\left(\frac{1}{\epsilon_{op}} - \frac{1}{\epsilon_s}\right) \tag{8}$$

the same sources cited above for ϵ_s. The radii of the donor, a_P, and acceptor, a_Q, were estimated using HyperChem (ver. 3.0). The radius of the quinone was evaluated as the average of the three cross-ring distances (oxygen−oxygen, hydrogen−hydrogen, and hydrogen-methylene carbon) and gave a value of $a_Q = 3.2 \pm 0.2$ Å. The radius of the porphyrin was taken as an average of the radius out to the edge of the pyrrole ring and the radius out to the tolyl methyl groups. A value of $a_P = 8 \pm 2.5$ Å was obtained. For all measurements, the atomic radii of the outer atoms were taken into account (atomic radii used: H, 0.37 Å; C, 0.77 Å; O, 0.73 Å). Given $\Delta G°$ and λ, the Franck−Condon factor can be determined. Thus, using the experimentally determined rate constants for the β-turn, the electronic coupling matrix, H_{ab}, was calculated from eq 1. Similar methods were used to evaluate $\Delta G°$, λ, and H_{ab} for the previously reported 5-(4-carboxyphenyl)-10,15,20-tri(*p*-tolyl)porphyrin-*N*-quinonyl-2-methylamide (PAQ) (a_{PQ} = 12.6 Å, assuming trans stereochemistry about the amide bond; range with Boltzmann weighting ≥0.1 is 12.5−12.9 Å).

Results

Structural characterization is of prime importance for interpretation of electron-transfer data in nonrigid donor−acceptor systems. Thus, we have carried out structural studies on Por/PL/DMB and tBoc/PL/DMB in chloromethanes and dimethyl sulfoxide using NMR and infrared spectroscopic methods. The data are compared with data for standard compounds as well as *N*-acetyl-L-proline-L-lactate-*N*-methylamide (Ac/PL/NHMe).[24] These comparisons have allowed determination of the importance of the capping groups on the conformation of the proline-lactate depsipeptide. The presence of a single amide NH in these compounds and carbonyl groups with very distinct stretching frequencies also has allowed detailed conformational analysis using these spectroscopic methods.

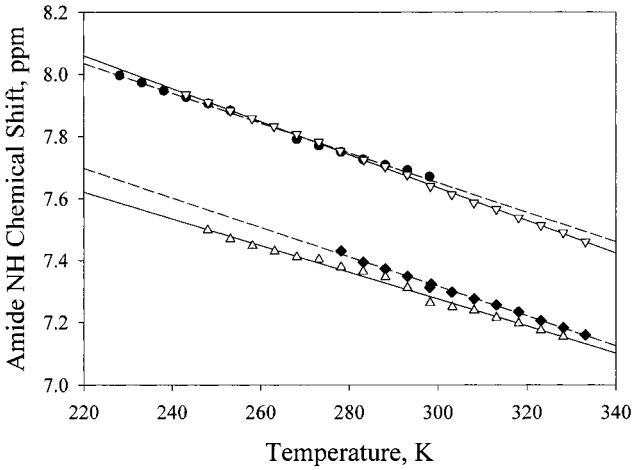

Figure 2. Temperature dependence of the ^{1}H NMR shifts of the amide NH for β-turn-forming compounds in chloromethane solvents: 1.0 mM tBoc/PL/DMB in $CDCl_3$ (▽, solid line); 1.36 mM Por/PL/DMB in CD_2Cl_2 (●, dashed line); 1.35 mM tBoc/PL/DMB in CCl_4 (△, solid line); 1.36 mM Por/PL/DMB in CCl_4 (◆, dashed line).

Table 1. Temperature Dependence of Amide NH NMR Resonances for β-Turn-Forming Compounds

compound	solvent	$\Delta\delta$NH/ΔT (ppb/K)
tBoc/PL/DMB	CCl_4	−4.33
Por/PL/DMB	CCl_4	−4.78
tBoc/PL/DMB	$CDCl_3$	−5.30
Ac/PL/NHMe[a]	CD_2Cl_2	−3.51
Por/PL/DMB	CD_2Cl_2	−4.79

[a] Data from ref 24a.

Structural and Thermodynamic Properties of Por/PL/DMB in Chloromethanes. Temperature-dependent NMR studies were carried out to assess the presence of the β-turn (C_{10}) conformation. The amide NH chemical shift was monitored from −25 to 60 °C in CCl_4, −30 to 60 °C in $CDCl_3$, and −45 to 25 °C in CD_2Cl_2. Por/PL/DMB was examined in CCl_4 and CD_2Cl_2, and tBoc/PL/DMB was examined in CCl_4 and $CDCl_3$ (see Figure 2). All four temperature-dependent experiments were compared to temperature-dependent NMR experiments on Ac/PL/NHMe[24a] in CD_2Cl_2 (see Table 1). The amide NH chemical shift could not be observed for the Por/PL/DMB in CD_2Cl_2 from −5 to −20 °C since the amide NH resonance was hidden by porphyrin resonances. The temperature ranges selected were limited by the melting and boiling points of the solvent.

A small value of the rate of change of the amide NH chemical shift with respect to temperature, $\Delta\delta$NH/ΔT, is typically associated with an amide NH which does not change hydrogen-bonding state significantly as a function of temperature. Gener-

(20) (a) Riddick, J. A.; Bunger, W. B. *Techniques of Chemistry II, Organic Solvents*, 4th ed.; Wiley-Interscience: New York, 1970; pp 348−349; (b) pp 466−467.

(21) Wuthrich, K. *NMR of Proteins and Nucleic Acids*; Wiley-Interscience: New York, 1986.

(22) Allinger, N. L. *J. Am. Chem. Soc.* **1977**, *99*, 8127−8134.

(23) (a) Opperman, K. A.; Mecklenburg, S. L.; Meyer, T. J. *Inorg. Chem.* **1994**, *33*, 5295−5301. (b) Hupp, J. T.; Neyhart, G. A.; Meyer, T. J.; Kober, E. M. *J. Phys. Chem.* **1992**, *96*, 10820−10830.

(24) (a) Liang, G.-B.; Rito, C. R.; Gellman, S. H. *J. Am. Chem. Soc.* **1992**, *114*, 4440−4442. (b) Boussard, G.; Marraud, M.; Neel, J. *Biopolymers* **1977**, *16*, 1033−1052.

ally, the lower the magnitude of $\Delta\delta NH/\Delta T$, the more complete hydrogen bonding is considered to be relative to that of other similar compounds in a given solvent.[25] As is evident in Figure 2 and Table 1, the data for tBoc/PL/DMB and Por/PL/DMB in chloromethane solvents show that the hydrogen-bonding state is not changing with a change in temperature, and that the addition of the porphyrin moiety does not strongly affect $\Delta\delta NH/\Delta T$. Similarly, the folding of the tBoc/PL/DMB β-turn in chloromethanes is not significantly affected by the addition of the dimethoxybenzene moiety when compared to the $\Delta\delta NH/\Delta T$ results from the depsipeptide, Ac/PL/NHMe.[24a] Ac/PL/NHMe is known to be essentially completely in a β-turn conformation in DCM.[24] The somewhat larger magnitude of $\Delta\delta NH/\Delta T$ for Por/PL/DMB in DCM may indicate a smaller equilibrium constant for β-turn formation.

Although the temperature dependence of the amide NH NMR resonance is suggestive, it is not definitive proof of hydrogen bonding, and thus the conformation was also assessed by infrared spectroscopy. In the amide A region (amide NH stretch, 3300−3500 cm^{-1}), the stretching frequency for the amide NH group depends on its environment. If the amide NH is involved in a hydrogen bond to a peptide carbonyl, then the stretch appears in the range 3300−3370 cm^{-1} in chloromethanes.[24,26] The non-hydrogen-bonding amide typically occurs around 3450 cm^{-1}.[24,26] In previously reported work, Por/PL/DMB was examined at room temperature to determine the relative amount of β-turn formed versus the non-hydrogen-bonded state.[14] The equilibrium constant for β-turn formation, $K_{\beta-turn}$, was found to be 5.7 (86% turn formation). Given that Ac/PL/NHMe is considered to be completely in a β-turn conformation under these conditions, the observation of 86% β-turn formation for Por/PL/DMB is consistent with the somewhat larger magnitude of $\Delta\delta NH/\Delta T$ observed above.

In the work reported here, the infrared spectrum of Por/PL/DMB was examined as a function of temperature to determine the temperature dependence of folding. The amide stretch of the non-hydrogen-bonding standard, NPMA, showed a slight temperature dependence of the molar absorptivity, ϵ. The molar absorptivity changes linearly, with a temperature coefficient of -0.28 M^{-1} cm^{-1} K^{-1} (from linear regression analysis, $\epsilon(T) = -0.28$ M^{-1} cm^{-1} $K^{-1}(T) + 205$ M^{-1} cm^{-1}; $r^2 = 0.982$ at 3445 cm^{-1}). Similar temperature dependences for the infrared absorptivity of non-hydrogen-bonded amides have been observed previously for *O*-acetyl-L-lactate-*N*-methylamide (Ac/L/NHMe)[27] and *N*-methylacetamide.[28] A concentration of 1.04 mM was used for NPMA to avoid intermolecular hydrogen bonding, which was evidenced by the absence of a hydrogen-bonded amide peak in the range of 3300−3370 cm^{-1}. The only peak present was the expected non-hydrogen-bonded amide NH near 3445 cm^{-1}. Lack of intermolecular hydrogen bonding at this concentration is typical for compounds of this type.[26c,27] Thus, Por/PL/DMB was examined over the same temperature range and at a similar concentration as for NPMA. At all temperatures, both hydrogen-bonded and non-hydrogen-bonded amide A IR absorbances were present (Figure 3A). The absorbance of the non-hydrogen-bonded amide was much lower than that for the hydrogen-bonded amide. Calculation of $K_{\beta-turn}$ (eq 3, Experimental Section) throughout the temperature range gave values from 6.3 to 5.7. Thus, the folding for the depsipeptide β-turn in Por/PL/DMB is almost temperature independent.

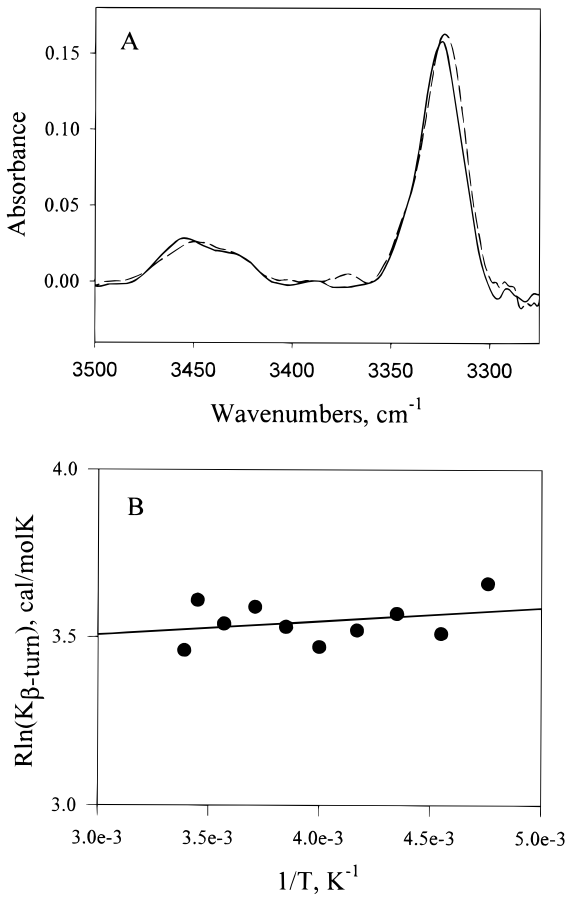

Figure 3. (A) Infrared spectra in the amide A (NH stretch) region for Por/PL/DMB at 210 (solid line) and 240 K (dashed line) at a concentration of 1.04 mM in CH_2Cl_2. The low broad peak near 3445 cm^{-1} is due to amide NH which is not hydrogen bonded. The sharp peak near 3325 cm^{-1} is due to amide NH involved in a hydrogen bond. (B) Van't Hoff plot using $K_{\beta-turn}$ values (eq 3, Experimental Section) extracted from amide A data.

A van't Hoff plot of the temperature-dependent infrared folding data can give insight into the driving force for the folding process (see Figure 3B). The van't Hoff analysis yields a linear plot within error, where the slope represents $-\Delta H°$ and the *y*-intercept is $\Delta S°$ for the folding process. A line where the slope approaches zero indicates that the folding process is driven not by enthalpy, but by entropy. For the β-turn-folding equilibrium of Por/PL/DMB in CH_2Cl_2, $\Delta H° = -0.04 \pm 0.05$ kcal/mol and $\Delta S° = 3.4 \pm 0.2$ eu. Thus, β-turn formation is entropically driven. Similar results have been observed for other β-turn-forming peptides.[24a]

A ROESY NMR experiment[16] was also carried out on Por/PL/DMB in CD_2Cl_2 in an attempt to obtain confirmatory structural data on the β-turn conformation. Since this is a depsipeptide, the amide NH between the $n + 1$ and $n + 2$ residues of the turn is replaced with an ester linkage. This NH normally has short through-space distances to the $C_\alpha H$ of the $n + 1$ (proline) and the amide NH of the $n + 3$ residue, which are characteristic of a β-turn.[21] Sometimes the $C_\alpha H$ ($n + 1$) to

(25) Dyson, H. J.; Rance, M.; Houghten, R. A.; Lerner, R. A.; Wright, P. E. *J. Mol. Biol.* **1988,** *201*, 161−200.

(26) (a) Haque, T. S.; Little, J. C.; Gellman, S. H. *J. Am. Chem. Soc.* **1994**, *116*, 4105−4106. (b) Haque, T. S.; Little, J. C.; Gellman, S. H. *J. Am. Chem. Soc.* **1996**, *118*, 6975−6985. (c) Liang, G.-B.; Rito, C. R.; Gellman, S. H. *Biopolymers* **1992**, *32*, 293−301.

(27) Gallo, E. A.; Gellman, S. H. *J. Am. Chem. Soc.* **1993**, *115*, 9774−9788.

(28) Gellman, S. H.; Dado, G. P.; Liang, G.-B.; Adams, B. R. *J. Am. Chem. Soc.* **1991**, *113*, 1164−1173.

amide NH ($n + 3$) cross-peak can be observed,[29] although the distance (3.3−3.6 Å) is at the edge of what can normally be observed in a ROESY NMR experiment, and it is often not detected.[21] This latter interaction is the only one characteristic of a β-turn which might be observable for Por/PL/DMB. It was not observed. The only cross-peaks observed for the amide NH of Por/PL/DMB were with the methylene hydrogens next to the amide NH and the closest aromatic ring hydrogen (very weak) on the dimethoxybenzene ring. Notably, no cross-peaks between the dimethoxybenzene ring and the prophyrin ring were observed. This is consistent with previously reported visible absorption data,[14] which indicate no electronic interaction between the porphyrin ring and the dimethoxybenzene ring in Por/PL/DMB or between the porphyrin ring and the quinone ring for Por/PL/Q. Thus, the ROESY NMR data confirm that there are no significantly populated conformations where the porphyrin and the dimethoxybenzene ring come in contact with each other.

Effects of Dimethyl Sulfoxide on the Structural Properties of Por/PL/DMB. The ability of Por/PL/DMB and tBoc/PL/DMB to form a β-turn was examined in the hydrogen bond-disrupting solvent DMSO as well. The NMR spectra of tBoc/PL/DMB and Por/PL/DMB were examined in DMSO-d_6 versus $CDCl_3$ and CD_2Cl_2 to determine the conformation in hydrogen-bonding versus non-hydrogen-bonding solvents. NMR spectra of both of these compounds in $CDCl_3$ and CD_2Cl_2 show no evidence of conformational heterogeneity, consistent with the predominance of the β-turn conformation. Clear evidence for disruption of hydrogen bonding can be seen for Por/PL/DMB and tBoc/PL/DMB in DMSO-d_6. Several proton resonances in both compounds are doubled, indicating two distinct conformations interconverting slowly on the NMR time scale. Notably, the tBoc methyl groups in tBoc/PL/DMB show one sharp singlet at 1.39 ppm in $CDCl_3$. In DMSO-d_6, the tBoc methyl groups are split into two peaks of approximately equal intensity, reflecting the presence of cis and trans isomers about the tertiary proline amide. The trans proline isomer is no longer locked in by β-turn formation.

To further characterize the hydrogen bonding of Por/PL/DMB in DMSO versus chloromethanes, infrared amide I spectroscopy was used. The amide I region of the infrared spectrum is due predominately to the C═O stretching vibration.[30] Since Por/PL/DMB has three different types of carbonyls (secondary amide, ester, and primary amide), which resonate at different frequencies, interpretation of the spectra is relatively straightforward. Figure 4A shows the IR spectrum of Por/PL/DMB in CH_2Cl_2. Four distinct absorbances can be seen at 1743.5 (proline ester), 1674.4 (secondary amide), 1619.5 (tertiary benzoyl amide), and 1607.5 cm^{-1} (aromatic ring vibrations). The assignments are based on studies of model compounds (see Table 2). Aromatic ring vibrations near 1605 cm^{-1} are observed for 2,5-dimethoxytoluene and for 5,10,15-tri(*p*-tolyl)-20-(*p*-methylbenzoate)porphyrin in both DCM and DMSO (data not shown). Interestingly, the tertiary benzoyl amide is shifted ∼12 cm^{-1} to lower energy compared to that of the standard compound, methyl-1-benzoyl-2-L-pyrrolidinecarboxylate (MBPC) (see Table 2). This shift is of the magnitude expected for the participation of this carbonyl in the hydrogen bond of a β-turn.[24b] Figure 4B shows the IR spectrum of Por/PL/DMB in DMSO. Clear differences are evident. The aromatic ring vibration peak (1604.9 cm^{-1}) is farther from the tertiary benzoyl amide peak (1629.9 cm^{-1}), such that it now appears as a low shoulder on this peak. The secondary amide peak is more complex, and the prolyl ester peak is broadened and less intense. Of note, the tertiary benzoyl amide is no longer shifted to lower energy,

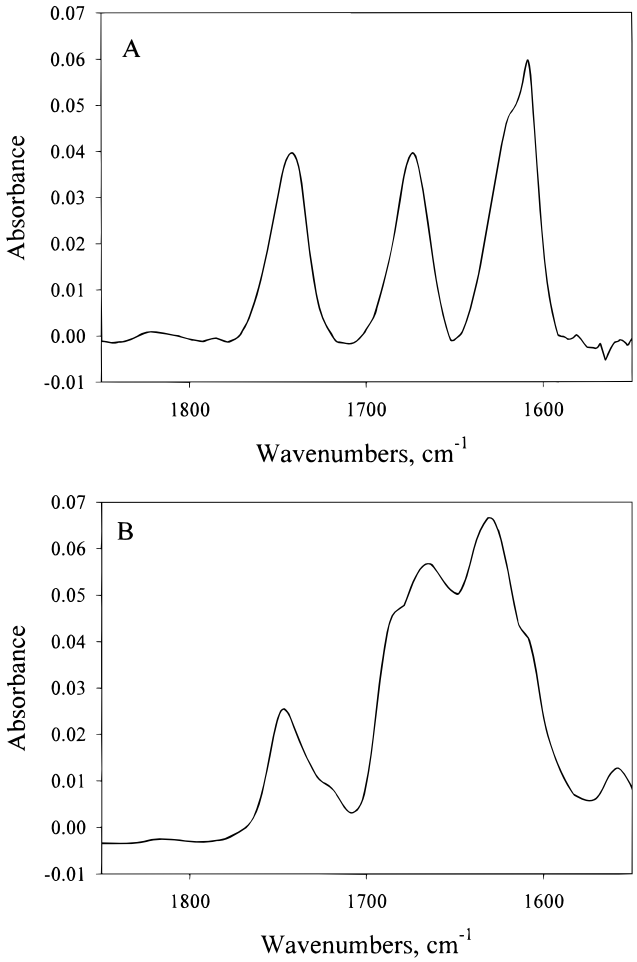

Figure 4. Amide I (C═O stretch) data for Por/PL/DMB. (A) Data acquired in DCM at a concentration of 1.89 mM and a temperature of 298 K. Curve-fitting analysis (see Experimental Section) yielded the following peak components: ester, 1743.5 cm^{-1}; 2° amide, 1674.4 cm^{-1}; 3° amide 1619.5 cm^{-1}; aromatic ring, 1607.5 cm^{-1}. (B) Data acquired in DMSO at a concentration of 0.67 mM and $T = 298$ K. Curve-fitting analysis yielded the following components: ester, 1747.5, 1731.3 cm^{-1}; 2° amide, 1688.0, 1667.0 cm^{-1}; 3° amide, 1629.9 cm^{-1}; aromatic ring, 1604.9 cm^{-1}.

Table 2. Amide I Infrared Vibrational Frequencies (in cm^{-1})

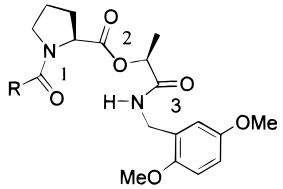

	DCM			DMSO		
compound	3° amide 1	ester 2	2° amide 3	3° amide 1	ester 2	2° amide 3
Por/PL/DMB[a]	1619.5	1743.5	1674.4	1629.9	1747.5	1667
					1731.3 (sh)	1688 (sh)
MAPC[b]	1646.0	1743.9		1645.0	1742.0	
MBPC[c]	1631.5	1744.0		1630.7	1742.9	

[a] R = 5-(*p*-phenyl)-10,15,20-tri(*p*-tolyl)prophyrin moiety. [b] R = methyl, ester 2 is a methyl ester. [c] R = phenyl, ester 2 is a methyl ester.

(29) Imperiali, B.; Fisher, S. L.; Moats, R. A.; Prins, T. J. *J. Am. Chem. Soc.* **1992**, *114*, 3182−3188.

(30) Krimm, S.; Bandekar, J. *Adv. Protein Chem.* **1986**, *38*, 181−364.

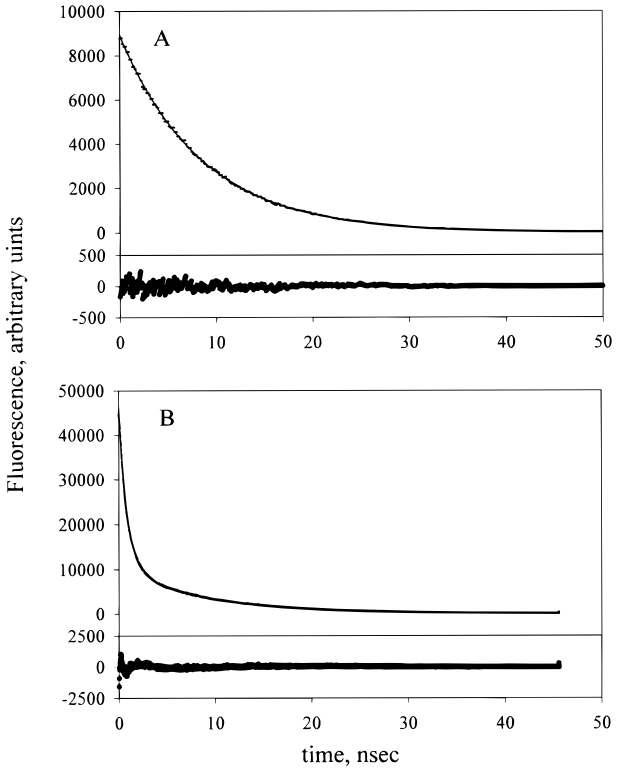

Figure 5. TCSPC data at 25 °C for Por/PL/DMB (A) and Por/PL/Q (B) in DCM. [Por/PL/DMB] = 8.9 μM. [Por/PL/Q] = 1.8 μM. The *y*-axis fluorescence intensity represents the number of counts per channel. Each channel has been converted to time in nanoseconds on the *x*-axis. Solid lines through the data points represent the fit to the data. The data in part A was fit to a single-exponential decay. The data in part B was fit to two exponential decays. Increasing the number of exponential decays in the fit for either data set did not significantly improve the fit. The residuals of each fit to the data are shown below the data.

as would be expected if it were hydrogen-bonded in a β-turn conformation. Its frequency is shifted only 1 cm^{-1} to lower energy relative to the non-hydrogen-bonding standard MBPC in DMSO (Table 2), indicating almost complete disruption of the β-turn hydrogen bond.

Fluorescence Lifetime Measurements. The photoinduced electron transfer between the excited state of the porphyrin and the quinone was monitored in dichloromethane by TCSPC fluorescence spectroscopy. In previous work, a reduction in the steady-state fluorescence of Por/PL/Q relative to Por/PL/DMB indicated electron transfer was competitive with the intrinsic emission lifetime.[14] Figure 5 compares the fluorescence decays for the excited states of Por/PL/DMB and Por/PL/Q in DCM. Clearly, the emission lifetime of Por/PL/Q is significantly shorter than that of Por/PL/DMB, consistent with a competitive electron-transfer process. The lifetimes extracted from curve-fitting analysis are reported in Table 3. From visual inspection of Figure 5B, it is clear that the fluorescence decay of Por/PL/Q is not monoexponential. The lifetime for the slower process (Table 3) is within error of that for Por/PL/DMB. Spectroscopic evaluation of the degree of oxidation of Por/PL/Q indicated that it was 91% oxidized (9% in the hydroquinone form, Por/PL/QH_2) for the lifetime data shown. This small quantity of Por/PL/QH_2, which is not competent for electron transfer, explains part of the amplitude with a lifetime within error of that for Por/PL/DMB. Since ~15% of Por/PL/Q is not in the β-turn conformation, a possible explanation of the additional amplitude with a lifetime similar to that of Por/PL/DMB is that electron transfer is not competitive with intrinsic fluorescence decay for Por/PL/Q in non-β-turn conformations.

Table 3. Fluorescence Lifetimes (in ns) for Por/PL/DMB and Por/PL/Q in DCM and DMSO[a]

	compound	
solvent	Por/PL/DMB	Por/PL/Q
DCM	8.95	8.76 (24%)[b] 0.85 (76%)[b]
DMSO	11.56	11.47 (94%)[b] 2.27 (6%)[b]

[a] Errors in the lifetimes are ±0.1 ns. [b] Percent amplitude for fluorescence emission decays that are not monoexponential.

Table 4. Electron-Transfer Rate Constants and Calculated Values for Driving Force, Solvent Reorganization Energy, and Electronic Coupling Matrix Element

compound, solvent	Por/PL/Q, DCM	Por/PL/Q, DMSO	PAQ,[a] DCM
k_{et} (s^{-1})[b]	$(1.1 \pm 0.1) \times 10^9$	$(3.5 \pm 0.2) \times 10^8$	$(8.0 \pm 0.4) \times 10^8$
$-\Delta G°$ (eV)[c]	0.67 ± 0.02	0.5 ± 0.1	0.63 ± 0.01
λ_s (eV)[d]	0.64 ± 0.06	0.73 ± 0.07	0.77 ± 0.01
H_{ab} (cm^{-1})[e]	2.4 ± 0.5	3 ± 2	3.1 ± 0.2

[a] k_{et} for PAQ is from ref 13. [b] k_{et} is calculated from eq 4 in the Experimental Section using the lifetime for Por/PL/DMB for τ_o and the fast lifetime for Por/PL/Q for τ_1. [c] Calculated using eq 5 in the Experimental Section. The error reflects the range of $-\Delta G°$ values due to the uncertainty in a_{PQ}. [d] Calculated using eq 8 in the Experimental Section. The error reflects the range of λ_s values due to the uncertainty in a_{PQ}. [e] H_{ab} was calculated using eq 1 and the values of $-\Delta G°$, λ_s, and k_{et} from this table. The error in H_{ab} reflects the range of H_{ab} values due to the errors in $-\Delta G°$ and λ_s resulting from the uncertainty in a_{PQ}. The values of a_P and a_Q cause errors in $-\Delta G°$ and λ_s which will affect the evaluation of H_{ab} as well. However, for comparison between PAQ and Por/PL/Q, the values of a_P and a_Q must be the same for each comparison. The most extreme effects occur when a_P and a_Q are both at the high or the low end of their error ranges. For $a_P = 10.7$ and $a_Q = 3.4$, the values of H_{ab} for the DCM data are as follow: Por/PL/Q, 1.9 ± 0.2 cm^{-1}; PAQ, 2.1 ± 0.1 cm^{-1}. For $a_P = 5.6$ and $a_Q = 3.0$, the values of H_{ab} for the DCM data are as follow: Por/PL/Q, 4 ± 1 cm^{-1}; PAQ, 6.2 ± 0.5 cm^{-1}.

To test this hypothesis, fluorescence lifetime measurements were also made in dimethyl sulfoxide. IR data presented above indicate that dimethyl sulfoxide nearly completely disrupts the β-turn hydrogen bond. Thus, excited-state quenching due to electron transfer will have to occur through the depsipeptide backbone (10 covalent bonds). The Por/PL/Q compound in DMSO gave a biexponential decay (Table 3). The major lifetime (94% of the amplitude) is essentially identical to the lifetime of Por/PL/DMB in DMSO (11.56 ns), indicating that electron transfer does not compete with fluorescence decay for the majority of Por/PL/Q conformations in DMSO. A minor fast component in the fluorescence decay is also resolved, suggesting that a small amount of β-turn conformation still persists in DMSO, consistent with the amide I IR data.

Electron-transfer rate constants, k_{et}, for Por/PL/Q in DCM and DSMO are collected in Table 4. Data for PAQ[12,13] are included for comparison. The large magnitude of the rate constant for Por/PL/Q suggests that electron transfer through the hydrogen bond interface of this compound is very efficient. Direct comparison of k_{et}, however, cannot be done between different solvents and different compounds to assess the efficiency of electronic coupling through the hydrogen bond interface. Variations in average donor−acceptor separation in different compounds and the solvent dielectric in different solvents will affect both the driving force and the reorganization energy for the electron-transfer reaction. To determine electronic coupling more accurately, changes in the Franck−Condon

factor for different electron-transfer reactions must be assessed. The driving force, $-\Delta G°$, the solvent reorganization, λ_s, and the electronic coupling matrix element, H_{ab}, calculated as described in the Experimental Section, are presented in Table 4. Qualitatively, this evaluation of H_{ab} is consistent with expectation. PAQ, with the shorter through-bond pathway (four bonds), has the larger value of H_{ab}. Por/PL/Q in DCM has the smaller value of H_{ab}, consistent with the longer through-bond pathway (six bonds).

Discussion

Structural Analysis of the Donor−Acceptor Compound Bridged by a Depsipeptide. Por/PL/Q is based on a well-studied depsipeptide, Ac/PL/NHMe, which is known to adopt essentially completely a β-turn conformation in chloromethanes.[24] Since the capping groups on the depsipeptide (PL) are significantly altered in Por/PL/DMB(Q), we carried out spectroscopic studies on Por/PL/DMB and its simpler analogue, tBoc/PL/DMB, to determine their structural propensities. We have used Por/PL/DMB rather than Por/PL/Q for structural studies because it is available in larger quantities and is more stable than Por/PL/Q. Modeling studies indicate that steric constraints prevent the oxygen atoms of either the quinone or dimethoxybenzene moieties from hydrogen bonding to the amide NH. Thus, Por/PL/DMB and Por/PL/Q should have similar structural properties.

Our data provide strong support for the presence of the β-turn in DCM. In the amide A region, the amide NH stretch is almost entirely shifted to the lower wavenumber region (3325 cm^{-1}), and only a small absorbance band remains at 3445 cm^{-1} in the region expected for a non-hydrogen-bonded amide (see Figure 3). In the amide I region, a shift of ∼12 cm^{-1} is observed for the 3° amide carbonyl of the benzoyl−proline linkage relative to the model compound, MBPC (see Table 2). A shift of this magnitude is typical for a 3° amide carbonyl involved in a hydrogen bond to an amide NH.[24b] No shift in the position of the prolyl ester amide I absorption of Por/PL/DMB (ester 2, in Table 2) relative to the model compounds MAPC and MBPC is observed, indicating the absence of a γ-turn. In support of this observation, *O*-Acetyl-L-lactyl-*N*-methylamide[24b] has only one amide A absorbance centered at 3469 cm^{-1}, indicating that the ester carbonyl to amide NH hydrogen bond needed to form a γ-turn in Por/PL/DMB is not very favorable. Thus, the β-turn structure involving the benzoylproline tertiary amide, within the limits of detection, is the only hydrogen-bonded conformation formed by Por/PL/DMB. The 120-cm^{-1} shift of the amide A band in the hydrogen-bonded state relative to the non-hydrogen-bonded state indicates that Por/PL/DMB forms a type I β-turn in DCM. For depsipetides, typically the type II β-turn results in an 80−90-cm^{-1} shift in the amide A frequency, whereas the type I β-turn produces a >100 cm^{-1} shift in the amide A frequency due to the shorter hydrogen bond distance (2.89 versus 2.97 Å O-to-N distance) in the type I depsipeptide β-turn.[24b] The hydrogen bond distance of Por/PL/Q of ∼2.89 Å is thus very close to the optimal distance of 2.8 Å used in the pathway model.[9]

From a thermodynamic standpoint, the type I β-turn formed by Por/PL/DMB is only weakly favored ($K_{\beta-turn} = 6.0$ and $\Delta G°_{\beta-turn} = -0.97$ kcal/mol at 0 °C). This corresponds to a β-turn population of about 85%, which is adequate for our purposes. $K_{\beta-turn}$ is essentially temperature independent, which is typical for β-turn-forming peptides and depsipeptides in chloromethanes.[24a] The similarity of the thermodynamic properties of Por/PL/DMB, tBoc/PL/DMB, and Ac-PL-NHMe[24] indicates that the steric bulk of the capping groups in proline-lactate depsipeptides has only a small impact on the β-turn propensity.

Conformational searches using HyperChem (see Experimental Section) indicate that the porphyrin and quinone moieties of Por/PL/Q cannot directly interact with each other in the β-turn conformation. Previously reported UV−vis spectroscopic studies of Por/PL/Q and Por/PL/DMB indicate no electronic interaction between the donor and acceptor chromophores.[14] The ROESY NMR data reported here confirm this previous observation. Porphyrin−quinone donor−acceptor compounds with flexible alkane spacers[31] have shown considerable electronic interaction between the donor and acceptor chromophores. Clearly, the relatively rigid conformation of the β-turn prevents such interactions. Thus, the fast electron-transfer event observed here for Por/PL/Q is not due to direct chromophore interaction, but results from the shorter electronic coupling pathway provided by the hydrogen bond of the β-turn.

Our data show that DMSO profoundly affects the conformation of Por/PL/DMB. Previous work indicates that DMSO disrupts hydrogen bonds in proteins and peptides.[26b,32] Both NMR and IR data show evidence of conformational heterogeneity. The IR data also indicate that the β-turn hydrogen bond has been nearly completely disrupted. The tertiary benzoyl−proline amide carbonyl stretch is now centered at ∼1630 cm^{-1}, only slightly less than the value observed for the model compound, MBPC (see Table 2).

Electron Transfer through a Hydrogen-Bonded β-Turn Interface. Por/PL/Q was designed such that the shortest through-bond electronic coupling pathway would require electronic coupling through a hydrogen bond. A number of donor−acceptor systems involving electron transfer across peptide bridges have been studied. Some variability in the decrease in electron-transfer rate per peptide unit has been reported. For short proline-bridged systems, the decrease in k_{et} tends to be on the order of 15−30-fold per proline unit.[4,33] For short proline bridges, a random conformation is expected. An electron-transfer rate of 8.0×10^8 s^{-1} in DCM has been reported for direct linkage via an amide bond of the donor and acceptor used in this study (PAQ, Figure 1 and Table 4). Thus, insertion of two bridging amino acid units would be expected to decrease k_{et} by a factor of ∼200−1000 for a random coil conformation. Electron transfer would thus not be expected to compete well with the intrinsic excited-state decay rate of the porphyrin ($k = 1/\tau_{DMB} = 1.1 \times 10^8$ s^{-1}) for Por/PL/Q in a random coil conformation. The presence of secondary structure, however, has been shown to significantly enhance the electronic coupling in longer polyproline-bridged systems.[4] In the case of Por/PL/Q, the formation of a β-turn is expected to provide a shorter through-hydrogen-bond electronic coupling pathway which could significantly enhance the electron-transfer rate (four covalent bonds + one hydrogen bond versus 10 covalent bonds in the absence of the hydrogen bond of the β-turn). Clearly,

(31) (a) Siemiarczuk, A.; McIntosh, A. R.; Ho, T.-F.; Stillman, M. J.; Roach, K. J.; Weedon, A. C.; Bolton, J. R.; Connolly, J. S. *J. Am. Chem. Soc*. **1983**, *105*, 7224−7230. (b) Ho, T.-F.; McIntosh, A. R.; Weedon, A. C. *Can. J. Chem*. **1984**, *62*, 967−974.

(32) (a) Hollosi, M.; Majer, Z.; Ronai, A. Z.; Magyar, A.; Medzihradszky, K.; Holly, S.; Perczel, A.; Fasman, G. D. *Biopolymers* **1994**, *34*, 177−184. (b) Jackson, M.; Mantsch, H. H. *Biochim. Biophys. Acta* **1991**, *1078*, 231−235.

(33) Cabana, L. A.; Schanze, K. S. In *Electron Transfer in Biology and the Solid State*; Johnson, M. K., King, R. B., Kurtz, D. M., Jr., Kutal, C., Norton, M. L., Scott, R. A., Eds.; ACS Advances in Chemistry Series 226; American Chemical Society: Washington, DC, 1990; pp 101−124.

electron transfer competes with excited-state decay, indicating that the presence of the β-turn conformation has the expected effect.

A recent study on electron transfer with pyrazolate-bridged iridium dimers[34] has shown that the electronic coupling can vary significantly as a function of conformation—as is clearly the case here—such that electron transfer occurs exclusively from a given conformation. However, as these authors point out, other factors, such as the reorganization energy, λ, change with conformation, also modulating k_{et}. Such effects are also expected for the random coil conformation relative to the β-turn conformation of Por/PL/Q. Electron transfer in the random coil conformation is not competitive with that from the β-turn conformation, not only because H_{ab} is expected to be smaller but also because ΔG° decreases in magnitude and λ increases in magnitude due to the longer average donor−acceptor separation expected in the random coil state of Por/PL/Q. Both these effects are expected to decrease the magnitude of the Franck−Condon factor in eq 1 and hence the magnitude of k_{et}. Thus, the noncompetitiveness of electron transfer from the random coil conformation relative to the β-turn conformation is not solely attributable to electronic coupling.

In any system where a conformational equilibrium exists between more than one state, the potential effect of the conformational equilibrium on the electron-transfer rate data must be considered.[1e] If the rate constants for the equilibration process are faster than the rate of electron transfer, then the apparent rate of electron transfer will be a conformationally weighted average of the electron-transfer rates from the various conformations.[35] Based on our IR data, the conformational equilibrium for Por/PL/DMB can be approximated as a two-state equilibrium involving a hydrogen-bonded type I β-turn and a non-hydrogen-bonded random coil structure. Recent studies[36] on the rates of formation of ordered secondary structure from random coil peptides indicate that β-hairpin structures form with time constants on the order of 1 μs and α-helices form with time constants of 100−200 ns. Since formation of an α-helix is expected to be limited by the rate of nucleation of the first turn of the helix, the time constant for formation of an isolated β-turn should be no faster than the rate of helix formation. In fact, the β-turn folding rate should be somewhat slower than the α-helix folding rate since helix-forming peptides have multiple possible nucleation sites, whereas an isolated β-turn has only one way to form.

Intrinsic fluorescence and electron transfer for Por/PL/Q occur in the 1−10-ns time range, a time scale that is 1−2 orders of magnitude faster than the time scale expected for the conformational equilibrium between the β-turn and random coil states of Por/PL/Q. When the conformational equilibrium between states is slow relative to intrinsic fluorescence and electron-transfer rates, each conformation is expected to produce a separate emission decay. If the intrinsic fluorescence lifetimes are assumed to be independent of conformation, the observed emission lifetimes for each state will be controlled by the electron-transfer rate from that state. The relative amplitudes of each exponential decay will be proportional to the fractional occupancy of that conformation. For a two-state equilibrium, such as the β-turn/random coil equilibrium, the time dependence of the porphyrin excited state would be given by eq 9, where

$$[Por^*]_{total}(t) = [Por^*]_{o,total}\left(\left(\frac{K_{\beta-turn}}{1+K_{\beta-turn}}\right)\exp^{-(k_f + k_{et,\beta-turn})t} + \left(\frac{1}{1+K_{\beta-turn}}\right)\exp^{-(k_f + k_{et,random})t}\right) \quad (9)$$

$[Por^*]_{o,total}$ is the total porphyrin emission intensity at $t = 0$, k_f is the intrinsic fluorescence decay rate constant, $k_{et,\beta-turn}$ and $k_{et,random}$ are the electron-transfer rate constants for the β-turn and random conformations, respectively, and $K_{\beta-turn}$ is the equilibrium constant for β-turn formation. Thus, for Por/PL/Q, two exponential decays are possible. If not all of the quinone is in the oxidized state, a third exponential due to Por/PL/QH_2 would be expected, too. Spectroscopic data indicated that the degree of oxidation of Por/PL/Q was 91% for the reported lifetime measurements. Thus, ~9% of the amplitude should have a lifetime close to that of Por/PL/DMB. Since 85% of Por/PL/Q is in the β-turn conformation, ~77% of Por/PL/Q is both oxidized and in the β-turn conformation in our sample. This is very close to the amplitude (76%) of the fast lifetime of Por/PL/Q (Table 3). The remaining ~13% of Por/PL/Q is both oxidized and in the non-hydrogen-bonded conformation. The combined population of the unoxidized and non-hydrogen-bonded states (~22%) is close to the amplitude (24%) of the slow lifetime of Por/PL/Q (see Table 3). This analysis indicates that k_{et} for the non-hydrogen-bonded conformation is not competitive with the intrinsic fluorescence decay of the porphyrin, and thus its lifetime is indistinguishable from the decay due to Por/PL/QH_2.

To confirm this amplitude analysis, we monitored the fluorescence decay of Por/PL/Q in DMSO. In this case, almost all of the amplitude has a lifetime coincident with that of Por/PL/DMB. Infrared studies in the amide I region indicate that the β-turn is nearly completely disrupted (Figure 4, Table 2). Thus, it would appear that electron transfer in the absence of the β-turn conformation does not compete with the intrinsic fluorescence decay. This confirms the assertion that the faster lifetime observed in DCM is due to electron transfer in the β-turn conformation and that electron transfer from non-β-turn conformations does not compete with the intrinsic fluorescence decay, resulting in a lifetime which is indistinguishable from that due to Por/PL/QH_2. The small residual fast lifetime in DMSO (6% of total amplitude) appears to be due to a small amount of residual β-turn conformation, since the electronic coupling matrix element, H_{ab}, calculated from k_{et} extracted from this lifetime is similar to that obtained for the β-turn conformation in DCM (see Table 4).

Electronic Coupling through a Hydrogen Bond versus a Covalent Bond. One model which has had some success in predicting electronic coupling in proteins in instances where the homogeneous barrier model[7,8] has proven inadequate is the pathway model of Beratan and Onuchic.[1a,d,e,9] In this model, it is assumed that the electronic coupling matrix element, H_{ab}, is proportional to the product of electronic coupling across three different types of orbital interactions—covalent bonds, hydrogen bonds, and through-space interactions (eq 10). $H_{ab}{}^o$ represents

$$H_{ab} = H_{ab}{}^o \prod_i \epsilon_c \prod_j \epsilon_{hb} \prod_k \epsilon_{ts} \quad (10)$$

coupling of the donor and acceptor orbitals to the orbitals of

(34) Kurnikov, I. V.; Zusman, L. D.; Kurnikova, M. G.; Farid, R. S.; Beratan, D. N. *J. Am. Chem. Soc*. **1997**, *119*, 5690−5700.

(35) (a) Hoffman, B. M.; Ratner, M. A.; Wallin, S. A. In *Electron Transfer in Biology and the Solid State*; Johnson, M. K., King, R. B., Kurtz, D. M., Jr., Kutal, C., Norton, M. L., Scott, R. A., Eds.; ACS Advances in Chemistry Series 226; American Chemical Society: Washington, DC, 1990; pp 125−146. (b) Hoffman, B. M.; Ratner, M. A. *J. Am. Chem. Soc*. **1987**, *109*, 6237−6243.

(36) (a) Eaton, W. A.; Munoz, V.; Thompson, P. A.; Chan, C.-K.; Hofrichter, J. *Curr. Opin. Struct. Biol*. **1997**, 7, 10−14. (b) Munoz, V.; Thompson, P. A.; Hofrichter, J.; Eaton, W. A. *Nature* **1997**, 390, 196−199.

the molecular bridge, and ϵ_c, ϵ_{hb} and ϵ_{ts} represent electronic coupling decay factors for covalent bonds, hydrogen bonds, and through-space interactions, respectively.[1e,9] The value of ϵ_c has been estimated to be 0.6, and ϵ_{hb} has been estimated to be equivalent to coupling across two covalent bonds for an optimal (2.8 Å) hydrogen bond ($\epsilon_{hb} = \epsilon_c^2 = 0.36$).[1e,9]

To facilitate estimation of ϵ_{hb}, we have calculated H_{ab} from our data (Table 4). The value of ϵ_{hb} can be estimated by comparison to previously reported data[13] for the compound PAQ (see Table 4). This compound has the donor and acceptor of Por/PL/Q directly connected via an amide linkage (see Figure 1). The covalent pathway between the donor and acceptor has four covalent bonds. Thus, the only difference in the covalent pathways of PAQ and Por/PL/Q is the insertion of a hydrogen bond. The value of ϵ_{hb} can be calculated from eq 11 without having to assign a value to ϵ_c, since the ratio of the two

$$\frac{H_{ab}(\text{Por/PL/Q},\beta\text{-turn})}{H_{ab}(\text{PAQ})} = \frac{(\epsilon_c)_4\epsilon_{hb}}{(\epsilon_c)^4} \qquad (11)$$

electronic coupling matrix elements is equal to ϵ_{hb}. Since three of the four covalent bonds in the dominant through-bond pathways for Por/PL/Q and PAQ (see Figure 1) are identical, the assumption that ϵ_c cancels exactly is not unreasonable. The emission lifetime data for Por/PL/Q and PAQ were obtained in the same solvents, and the donor porphyrin and acceptor quinone are the same, also making this an appealing comparison. We obtain a value for ϵ_{hb} of 0.77 using eq 11. When the error in H_{ab} resulting from the uncertainties in a_{PQ}, a_P, and a_Q (see Table 4, footnote *e*) is accounted for the range of values obtained for ϵ_{hb} is 0.44−1.04. Thus, 0.8 ± 0.4 provides a reasonable experimental estimate for ϵ_{hb}. There will be additional error in our evaluation of ϵ_{hb} since we have ignored possible interference effects[37] from the completely covalent 10-bond pathway along the backbone of Por/PL/Q (see Figure 1). We expect this effect to be small relative to other sources of error. Our experimental value for ϵ_{hb} compares well to that of 0.51 reported by Therien and co-workers for electron transfer across a carboxylic acid hydrogen bond interface.[10a]

The amide NH- - -O═C hydrogen bond is the most prevalent hydrogen bond in proteins. Significantly, the value of ϵ_{hb} we report here for this type of hydrogen bond is of the order of magnitude predicted theoretically and provides direct evidence that the hydrogen bond networks provided by protein secondary structure can efficiently mediate electronic coupling. A key component of the efficiency of electronic coupling across the amide NH- - -O═C hydrogen bond likely results from the very weak acidity of the donor NH and the very weak basicity of the acceptor C═O. The Franck−Condon barrier due to proton motion during electron transfer is expected to be minimal in this case.[10c,d]

Comparison with Protein Systems and β-Sheet Mimics. A significant body of work exists on electron transfer in β-sheet proteins.[1d,e,38,39] Results on the distance dependence of electron transfer in peptide β-sheet mimics have also recently been reported.[5b] To a first approximation, k_{et} from the protein and peptide systems all show the same distance dependence for electron transfer ($\beta \sim 1.1$ Å^{-1}),[1d,e,5b,38b] indicating that electronic coupling is similar in all of these systems and particular to the secondary structure involved.[1d,e,38b] The surprising result from work with the blue copper protein, azurin,[1d,e,38,39] is that the log(k_{et}) versus distance dependence data for electron transfer along different β-strands all fall on the same line.[1e,38b] However, the β-strand extending out from the copper ligand, Cys 112, is expected to be more strongly coupled to the copper center due to the stronger electronic interaction of this ligand with the copper center.[1e,38] The explanation provided for the observed data was that hydrogen bonds in β-sheets provide electronic coupling similar to that of a covalent bond ($\epsilon_{hb} = \epsilon_c^2$), allowing electron transfer from all β-strands to couple through Cys 112.[1e,38] The data from our β-turn model system indicate that this is the case for peptide hydrogen bonds and supports the notion that hydrogen bonds of protein secondary structure are crucial for efficient electronic coupling in proteins.

Conclusions

We have evaluated the electronic coupling across the hydrogen bond of a β-turn using a porphyrin−quinone donor−acceptor compound bridged by a depsipeptide. Qualitatively, the data demonstrate that the hydrogen bond of a β-turn can provide efficient electronic coupling since a very large rate constant for electron transfer ($k_{et} = 1.1 \times 10^9$ s^{-1}) is observed in the β-turn conformation. A quantitative assessment of the coupling efficiency yielded a value of $\epsilon_{hb} = 0.8 \pm 0.4$, indicating that peptide hydrogen bonds are efficient electron-transfer mediators. This value for ϵ_{hb} is of the same order of magnitude as the theoretically predicted value of 0.36,[9] it agrees well with a previous estimate of $\epsilon_{hb} = 0.51$ for a carboxylic acid hydrogen bond interface,[10a] and it is consistent with other results indicating efficient electron transfer across hydrogen-bonded interfaces.[10b,c,d]

Acknowledgment. We thank Mike Machczynski and Jay Winkler at the Beckman Institute's Laser Resource Center (California Institute of Technology; Pasadena, CA) for their willingness to help with the TCSPC fluorescence lifetime work. We also thank Art Pardi at the Department of Chemistry and Biochemistry at the University of Colorado at Boulder for help with ROESY NMR experiments and Julanna Gilbert at the University of Denver for use of FT-IR instrumentation. Acknowledgment is made to the donors of the Petroleum Research Fund, administered by the American Chemical Society, for support of this research.

JA981384K

(37) (a) Skourtis, S. S.; Onuchic, J. N.; Beratan, D. N. *Inorg. Chim. Acta* **1996**, *243*, 167−175. (b) Skourtis, S. S.; Beratan, D. N. *J. Phys. Chem. B* **1997**, *101*, 1215−1234.

(38) (a) Regan, J. J.; Di Bilio, A. J.; Langen, R.; Skov, L. K.; Gray, H. B.; Onuchic, J. N. *Chem. Biol*. **1995**, *2*, 489−496. (b) Langen, R.; Colon, J. L.; Casimiro, D. R.; Karpishin, T. B.; Winkler, J. R.; Gray, H. B. *J. Biol. Inorg. Chem.* **1996**, *1*, 221−225.

(39) (a) Farver, O.; Pecht, I. *Biophys. Chem.* **1994**, *50*, 203−216. (b) Farver, O.; Skov, L. K.; Gilardi, G.; van Pouderoyen, G.; Canters, G. W.; Wherland, S.; Pecht, I. *Chem. Phys*. **1996**, *204*, 271−277. (c) Farver, O.; Bonander, N.; Skov, L. K.; Pecht, I. *Inorg. Chim. Acta* **1996**, *243*, 127−133.